



Synthetic conjugates of genistein affecting proliferation and mitosis of cancer cells

Aleksandra Rusin^{a,*}, Jadwiga Zawisza-Puchałka^b, Katarzyna Kujawa^a, Agnieszka Gogler-Piğłowska^a, Joanna Wietrzyk^c, Marta Świtalska^c, Magdalena Głowała-Kosińska^a, Aleksandra Gruca^b, Wiesław Szeja^b, Zdzisław Krawczyk^{a,b}, Grzegorz Gryniewicz^d

^a Department of Tumor Biology, Maria Skłodowska-Curie Memorial Cancer Center and the Institute of Oncology, Wybrzeże AK 15, 44-100 Gliwice, Poland

^b Silesian University of Technology, Krzywoustego 8, 44-100 Gliwice, Poland

^c Institute of Immunology and Experimental Therapy Polish Academy of Sciences, Weigla 12, 53-114, Poland

^d Pharmaceutical Research Institute, Rydygiera 8, 01-793 Warsaw, Poland

ARTICLE INFO

Article history:

Received 16 September 2010

Revised 4 November 2010

Accepted 8 November 2010

Available online 11 November 2010

Keywords:

Genistein glycoconjugates

Antiproliferative activity

Cell cycle

Mitotic spindle

Apoptosis

ABSTRACT

This paper describes the synthesis and antiproliferative activity of conjugates of genistein (**1**) and unsaturated pyranosides. Constructs linking genistein with a sugar moiety through an alkyl chain were obtained in a two-step synthesis: in a first step genistein was converted into an intermediate bearing an ω -hydroxyalkyl substituent, containing two, three or five carbon atoms, at position 7, while the second step involved Ferrier glycosylation reaction, employing glycals. Antiproliferative activity of several genistein derivatives was tested in cancer cell lines in vitro. The most potent derivative, **Ram-3** inhibited the cell cycle, interacted with mitotic spindles and caused apoptotic cell death. Neither genistein nor the sugar alone were able to influence the mitotic spindle organization. Our results indicate, that conjugation of genistein with certain sugars may render the interaction of derivatives with new molecular targets.

© 2010 Elsevier Ltd. All rights reserved.

1. Introduction

Genistein (**1**) is a phytochemical with widely demonstrated beneficial effects for human health.¹ Due to remarkable similarity in chemical structure to estrogen and its ability for binding to the estrogen receptor genistein is classified as a natural selective estrogen receptor modulator.^{2,3} Genistein aglycone might be a new potential therapy for the management of postmenopausal osteoporosis in humans combining a powerful bone-forming as well as an antiresorptive activity.⁴ In addition, hundreds of scientific publications report its wide range of nonhormonal activities, many of which have profound implications for cell function. Among the targets inhibiting cancer cell growth topoisomerase II, tyrosine kinases, the transforming growth factor- β (TGF β) signaling pathway and nuclear transcription factor NF- κ B are indicated.⁵ Genistein may be also useful in treatment of inherited metabolic diseases, such as mucopolysaccharidoses, due to influencing an epidermal growth factor-dependent pathway.⁶

In order to enhance the pharmacological potential of genistein several groups functionalized the molecule and found among plenty of synthetic derivatives several, which were active at

concentration one order of magnitude lower than a parent compound, or even affecting a new target.⁷ Current paper is a continuation of our previous work⁸ on glycosylation as an option for enhancement antiproliferative potential of genistein due to targeting mitotic spindles.

In plants, in which genistein is produced, it exists mainly in a glycosylated form, genistin⁹ which increases isoflavonoid solubility and stability.¹⁰ Although the main form of consumed genistein is its glycoside, genistin, and the only form transported through enterocytes to blood vessels in human is aglycon,^{11,12} there is no significant difference between bioavailability of genistein consumed in the form of aglycon or a glycoside, because of efficient deconjugation of the latter in the digestive tract.¹² After absorption, genistein is metabolized mostly to glucuronate and sulfate conjugates.¹³

While it is well documented that aglycon form of genistein can affect various cellular processes, much less is known about the biological activity of its glycoderivatives. Genistein glucuronides have been shown to have weak estrogenic activity and capability of in vitro activation of human natural killer cells^{14,15} and genistein 7-O- β -maltosides and 7-O- β -maltotriosides showed potent inhibitory effects on histamine release from rat peritonea mast cells.¹⁶ A highly relevant were findings that several semi-synthetic genistein glycosides could exert significant antiproliferative activity against different cancer cell lines.^{8,17,18}

* Corresponding author. Tel.: +48 32 278 98 44; fax: +48 32 278 98 40.

E-mail address: arusin@io.gliwice.pl (A. Rusin).

Preliminary estimation of the structure–activity relationship led to the conclusion that lipophilic glycosides are much more active than hydrophilic ones, however, the lipophilicity is not the only parameter influencing the activity of a molecule.¹⁷ There is a strong suggestion that the sugar moiety plays a key role for the biological activity of the genistein derivative, since one of the described glycosides, named G21, affected microtubule array, similarly to mitotic poisons.⁸ In the presented study we report the synthesis of new compounds linking genistein with an unsaturated pyranoside through an alkyl chain and describe their antiproliferative activity against cancer cell lines, corroborating the working hypothesis, that unsaturated sugar is a carrier of certain structural features reflected in antiproliferative activity of genistein conjugates.

2. Material and methods

2.1. Synthesis of genistein derivatives

2.1.1. General

The reagents (chemicals), all being of A.R. grade, were purchased from Across Organic. Genistein (**1**) (>96%) provided by Pharmaceutical Research Institute (Warsaw, Poland) was further refined by recrystallization from ethanol, which afforded pale yellow needles, mp: 298–299 °C.

Reactions and the resulted products were monitored by thin-layer chromatography (TLC) on Merck pre-coated silica gel F254 plates with separated compounds visualized at 254 nm under a UV lamp. Melting points (uncorrected) were determined with MTT-2 model. ESI mass spectra were obtained on a Mariner System 5304 mass spectrometer, and ¹H NMR spectra were recorded in DMSO-*d*₆ or CDCl₃ on a Varian (300 MHz) spectrometer with solvent signals allotted as internal standard. Sonication was performed in a ultrasonic cleaner Sonorex Super with irradiation delivered at 35 kHz and 500 W. Hydroxyalkylgenistein intermediates were recrystallised from methanol. Glycoconjugates were purified by column chromatography (Silica Gel 60, 70–230 mesh, Merck) and eluted with chloroform. Chromatographic fractions were pooled according to TLC analysis and solvents were evaporated under diminished pressure in rotary evaporators.

2.1.2. Chemistry

2.1.2.1. General procedure for preparation 7-O-ω-hydroxyalkylgenistein. Tetrabutylammonium salt of genistein (**2**) (10 mM) and alcohol (2-bromo-1-ethanol or 3-bromo-1-propanol, 11 mM) in 50 mL of dry DMF were stirred at temperature 50 °C for 24 h. After the completion of reaction, the mixture was diluted with 250 mL of ice water to form yellow solid. Recrystallization of the solid from 100 mL hot methanol gave product **3a** or **3b**.

5-Hydroksy-7-(2-hydroxyethyl)-3-(4-hydroksyphenyl)chromen-4-one (3a). Obtained after recrystallization as a white solid, in 88% yield; mp 219–221 °C; ¹H NMR δ (DMSO-*d*₆): 3.70–3.78 (m; 2H; –CH₂O–); 4.11 (t; 2H; J = 9.6 Hz; –CH₂O–); 4.97 (br s; 1H; –CH₂OH); 6.40, 6.65 (2 × d; 2H; J = 2.2 Hz; H-6, H-8); 6.83 (d; 2H; J = 8.7 Hz; H-3', H-5'); 7.39 (d; 2H; J = 8.7 Hz; H-2', H-6'); 8.40 (s; 1H; H-2); 9.63 (br s; 1H; 4'-OH); 12.96 (s; 1H; 5-OH). HRMS (ESI) Calcd C₁₇H₁₄O₆ [M+Na]⁺ 337.0682. Found 337.0666.

5-Hydroksy-7-(3-hydroxypropyl)-3-(4-hydroksyphenyl)chromen-4-one (3b). Obtained after recrystallization as a white solid, in 89% yield; mp 201–203 °C; ¹H NMR δ (DMSO-*d*₆): 1.84–1.92 (m; 2H; –CH₂–); 3.54–3.59 (m; 2H; –CH₂O–); 4.16 (dd; 2H; J = 6.2 Hz, J = 6.4 Hz; –CH₂OH); 4.62 (t; 1H; J = 6.4 Hz; –CH₂OH); 6.39, 6.65 (2 × d; 2H; J = 2.2 Hz; H-6, H-8); 6.83 (d; 2H; J = 8.6 Hz; H-3', H-5'); 7.39 (d; 2H; J = 8.6 Hz; H-2', H-6'); 8.41 (s; 1H; H-2); 9.64 (br s; 1H; 4'-OH); 12.96 (s; 1H; 5-OH). HRMS (ESI) Calcd C₁₈H₁₆O₆ [M+Na]⁺ 351.0839. Found 351.0833.

2.1.2.2. Procedure for preparation 7-O-(5-hydroxypentyl)genistein. Tetrabutylammonium salt of genistein **2** (10 mM) and 5-bromopentyl acetate (11 mM) in 50 mL of dry DMF were stirred at temperature 50 °C for 24 h. After the completion of reaction, the mixture was diluted with 250 mL of ice water to form yellow solid. Recrystallization of the solid from 100 mL hot methanol gave acylated product (**3c**). This acylated product (5 mM) and magnesium shavings in 50 mL of dry methanol were stirred at temperature 40 °C for 24 h. After the completion of reaction, the mixture was neutralized with an Amberlyst 15 followed by filtration. The filtrate was distilled to form white solid. Recrystallization of the solid from 100 mL hot methanol gave product **3d**.

5-Hydroksy-7-(5-hydroxypentyl)-3-(4-hydroksyphenyl)chromen-4-one (3d). Obtained after recrystallization as a white solid, in 88% yield; mp 154–157 °C; ¹H NMR δ (DMSO-*d*₆): 1.42–1.50 (m; 4H; 2 × –CH₂–); 1.71–1.76 (m; 2H; –CH₂–); 3.42 (q; 2H; J = 5.1 Hz; –CH₂OH–); 4.09 (t; 2H; J = 6.6 Hz; –CH₂O–); 4.40 (t; 1H; J = 5.1 Hz; –CH₂OH); 6.39, 6.64 (2 × d; 2H; J = 2.2 Hz; H-6, H-8); 6.83 (d; 2H; J = 8.7 Hz; H-3', H-5'); 7.39 (d; 2H; J = 8.7 Hz; H-2', H-6'); 8.40 (s; 1H; H-2); 9.62 (s; 1H; 4'-OH); 12.95 (s; 1H; 5-OH). HRMS (ESI) Calcd C₂₀H₂₀O₆ [M+Na]⁺ 379.1152. Found 379.1163.

2.1.2.3. General procedure for synthesis of 2,3-unsaturated pyranosides. To a solution of glycal (**4**, **5**, **6**) (0.2 mM) in anhydrous acetonitrile (40 mL) the aglycone (**3a**, **3b**, **3d**) (0.2 mM) and anhydrous InCl₃ (0.02 mM) was added. The contents were stirred at temperature 25 °C for 2 h and the reaction monitored by TLC (CHCl₃/MeOH = 10:1 (v/v)). The reaction mixture was quenched by the addition of aqueous sodium hydrogen carbonate (10%, 25 mL), extracted with dichloromethane (3 × 25 mL), dried over anhydrous sodium sulfate, filtered and washed with dichloromethane, and the combined organic extract was concentrated under vacuum. The residue was purified by column chromatography (CHCl₃) on silica gel to obtain the product.

5-Hydroksy-7-[(4,6-di-O-acetyl-2,3-dideoxy-α-D-erythro-hex-2-enopyranosyl)-2-O-ethyl]-3-(4-hydroksyphenyl)chromen-4-one (7a). Obtained after chromatography as colorless syrup, in 49% yield; ¹H NMR (CDCl₃) δ: 2.10 (s; 3H; AcO); 2.12 (s; 3H; AcO); 3.9–3.97 (m; 1H; H-5); 4.08–4.32 (m; 6H; 2 × –CH₂O–; H-6a, H-6b); 5.15 (br s; 1H; H-1); 5.36 (dd; 1H; J = 9.7 Hz; J = 1.3 Hz; H-4); 5.86–5.95 (m; 2H; H-2, H-3); 6.41, 6.38 (2 × d; 2H; J = 2.3 Hz; H-8g, H-6g); 6.61 (br s; 1H; 4'-OHg); 6.85 (d; 2H; J = 8.6 Hz; H-3'g, H-5'g); 7.34 (d; 2H; J = 8.6 Hz; H-2'g, H-6'g); 7.85 (s; 1H; H-2g); 12.83 (s; 1H; 5-OHg). HRMS (ESI) Calcd C₂₇H₂₆O₁₁ [M+Na]⁺ 549.1367. Found 549.1369.

5-Hydroksy-7-[(4,6-di-O-acetyl-2,3-dideoxy-α-D-erythro-hex-2-enopyranosyl)-3-O-propyl]-3-(4-hydroksyphenyl)chromen-4-one (7b). Obtained after chromatography as colorless syrup, in 65% yield; ¹H NMR (CDCl₃) δ: 2.04–2.19 (m; 2H; –CH₂–); 2.09 (s; 3H; AcO); 2.11 (s; 3H; AcO); 3.71 (dt; 1H; J = 9.9 Hz; J = 6.1 Hz; –CH₂O–); 3.98 (dt; 1H; J = 9.9 Hz; J = 6.1 Hz; –CH₂O); 4.04–4.16 (m; 3H; H-5; –CH₂O–); 4.17 (dd; 1H; J = 12.1 Hz; J = 2.6 Hz; H-6b); 4.25 (dd; 1H; J = 12.1 Hz; J = 5.3 Hz; H-6a); 5.06 (br s; 1H; H-1); 5.33 (dd; 1H; J = 9.7 Hz; J = 1.5 Hz; H-4); 5.85 (ddd; 1H; J = 10.2 Hz; J = 2.4 Hz; J = 1.8 Hz; H-3); 5.91 (dd; 1H; J = 10.2 Hz; J = 1.1 Hz; H-2); 6.37, 6.40 (2 × d; 2H; J = 2.4 Hz; H-6g, H-8g); 6.61 (br s; 1H; 4'-OHg); 6.85 (d; 2H; J = 8.6 Hz; H-3'g, H-5'g); 7.34 (d; 2H; J = 8.6 Hz; H-2'g, H-6'g); 7.84 (s; 1H; H-2g); 12.83 (s; 1H; 5-OHg). HRMS (ESI) Calcd C₂₈H₂₈O₁₁ [M+Na]⁺ 563.1523. Found 563.1531.

5-Hydroksy-7-[(4,6-di-O-acetyl-2,3-dideoxy-α-D-erythro-hex-2-enopyranosyl)-5-O-pentyl]-3-(4-hydroksyphenyl)chromen-4-one (7d). Obtained after chromatography as colorless syrup, in 48% yield; ¹H NMR (CDCl₃) δ: 1.51–1.64 (m; 2H; –CH₂–); 1.66–1.76 (m; 2H; –CH₂–); 1.79–1.89 (m; 2H; –CH₂–); 2.10 (s; 3H; AcO); 2.11 (s; 3H; AcO); 3.55 (dt; 1H; J = 9.7 Hz; –CH₂O–); 3.83 (dt; 1H; J = 9.7 Hz; –CH₂O–); 4.02 (dd; 2H; –CH₂O–); 4.09–4.18 (m; 1H;

H-5); 4.20 (dd; 1H; $J = 12.1$ Hz; $J = 2.6$ Hz; H-6b); 4.27 (dd; 1H; $J = 12.1$ Hz; $J = 5.1$ Hz; H-6a); 5.05 (br s; 1H; H-1); 5.33 (dd; 1H; $J = 9.7$ Hz; $J = 1.5$ Hz; H-4); 5.85 (ddd; 1H; $J = 11.2$ Hz; $J = 1.5$ Hz; $J = 1.8$ Hz; H-3); 5.91 (d; 1H; $J = 11.2$ Hz; H-2); 6.35, 6.38 (2 × d; 2H; $J = 2.2$ Hz; H-8g, H-6g); 6.86 (d; 2H; $J = 8.6$ Hz; H-3'g; H-5'g); 7.36 (d; 2H; $J = 8.6$ Hz; H-2'g; H-6'g); 7.84 (s; 1H; H-2g); 12.80 (s; 1H; 5-OHg). HRMS (ESI) Calcd $C_{30}H_{32}O_{11}$ [M+Na]⁺ 591.1837. Found 591.1841.

5-Hydroksy-7-[(4-O-acetyl-2,3,6-trideoxy- α -L-erythro-hex-2-enopyranosyl)-2-O-ethyl]-3-(4-hydroksyphenyl)chromen-4-one (8a). Obtained after chromatography as colorless syrup, in 54% yield; ¹H NMR (CDCl₃) δ : 1.25 (d; 3H; $J = 6.22$ Hz; H-6); 2.10 (s; 3H; AcO); 3.90–4.26 (m; 5H; H-5, 2 × -CH₂O-); 5.06–5.10 (m; 2H; H-1, H-4); 5.86–5.89 (m; 2H; H-2, H-3); 6.23 (br s; 1H; 4'-OHg); 6.39, 6.42 (2 × d; 2H; $J = 2.4$ Hz; H-8g, H-6g); 6.86 (d; 2H; $J = 8.6$ Hz; H-3'g, H-5'g); 7.35 (d; 2H; $J = 8.6$ Hz; H-2'g, H-6'g); 7.86 (s; 1H; H-2g); 12.83 (s; 1H; 5-OHg). HRMS (ESI) Calcd $C_{25}H_{14}O_9$ [M+Na]⁺ 491.1313. Found 491.1324.

5-Hydroksy-7-[(4-O-acetyl-2,3,6-trideoxy- α -L-erythro-hex-2-enopyranosyl)-3-O-propyl]-3-(4-hydroksyphenyl)chromen-4-one (8b). Obtained after chromatography as colorless syrup, in 86% yield; ¹H NMR (CDCl₃) δ : 1.20 (d; 3H; $J = 6.0$ Hz; H-6); 2.05–2.14 (m; 2H; -CH₂-); 2.09 (s; 3H; AcO); 3.68 (dt; 1H; $J = 9.9$ Hz; $J = 6.2$ Hz; -CH₂O-); 3.91–4.01 (m; 2H; H-5, -CH₂O-); 4.11–4.17 (m; 2H; -CH₂O-); 4.99 (br s; 1H; H-1); 5.05 (dd; 1H; $J = 9.3$ Hz; $J = 1.5$ Hz; H-4); 5.22 (br s; 1H; 4'-OHg); 5.80 (ddd; 1H; $J = 10.8$ Hz; $J = 2.4$ Hz; $J = 1.5$ Hz; H-3); 5.87 (d; 1H; $J = 10.8$ Hz; H-2); 6.39, 6.41 (2 × d; 2H; $J = 2.1$ Hz; H-8g, H-6g); 6.89 (d; 2H; $J = 8.7$ Hz; H-3'g, H-5'g); 7.39 (d; 2H; $J = 8.7$ Hz; H-2'g, H-6'g); 7.86 (s; 1H; H-2g); 12.83 (s; 1H; 5-OHg). HRMS (ESI) Calcd $C_{26}H_{26}O_9$ [M+Na]⁺ 505.1469. Found 505.1485.

5-Hydroksy-7-[(4-O-acetyl-2,3,6-trideoxy- α -L-erythro-hex-2-enopyranosyl)-5-O-pentyl]-3-(4-hydroksyphenyl)chromen-4-one (8d). Obtained after chromatography as colorless syrup, in 55% yield; ¹H NMR (CDCl₃) δ : 1.24 (d; 3H; $J = 6.3$ Hz; H-6); 1.53–1.74 (m; 4H; 2 × -CH₂-); 1.80–1.90 (m; 2H; -CH₂-); 2.10 (s; 3H; AcO); 3.53 (dt; 1H; $J = 9.6$ Hz; $J = 6.1$ Hz; -CH₂O-); 3.82 (dt; 1H; $J = 9.6$ Hz; $J = 6.6$ Hz; -CH₂O-) 3.96–4.05 (m; 3H; H-5, -CH₂O-); 4.97 (br s; 1H; H-1); 5.06 (dd; 1H; $J = 9.3$ Hz; $J = 1.5$ Hz; H-4); 5.22 (br s; 1H; 4'-OHg); 5.81 (ddd; 1H; $J = 10.5$ Hz; $J = 2.4$ Hz; $J = 1.5$ Hz; H-3); 5.87 (d; 1H; $J = 10.5$ Hz; H-2); 6.37, 6.39 (2 × d; 2H; $J = 2.2$ Hz; H-8g, H-6g); 6.89 (d; 2H; $J = 8.4$ Hz; H-3'g, H-5'g); 7.40 (d; 2H; $J = 8.4$ Hz; H-2'g, H-6'g); 7.85 (s; 1H; H-2g); 12.82 (s; 1H; 5-OHg). HRMS (ESI) Calcd $C_{28}H_{30}O_9$ [M+Na]⁺ 533.1782. Found 533.1806.

5-Hydroksy-7-[(4-O-(2,3,4,6-tetra-O-acetyl- β -D-galactopyranosyl)-6-O-acetyl-2,3-dideoxy- α -D-erythro-hex-2-enopyranosyl)-2-O-ethyl]-3-(4-hydroksyphenyl)chromen-4-one (9a). Obtained after chromatography as colorless syrup, in 67% yield; ¹H NMR (CDCl₃) δ : 1.98 (s; 3H; AcO); 2.05 (s; 3H; AcO); 2.08 (s; 3H; AcO); 2.12 (s; 3H; AcO); 2.16 (s; 3H; AcO); 3.89–4.35 (m; 11H; H-4, H-5, H-5', H-6a, H-6b, H-6a', H-6b'; 2 × CH₂O); 4.58 (d; 1H; $J = 8.2$ Hz; H-1'); 5.02 (dt; 1H; $J = 10.6$ Hz; $J = 3.5$ Hz; H-3'); 5.09 (d; 1H; $J = 1.1$ Hz; H-1); 5.21 (dd; 1H; $J = 10.6$ Hz; $J = 8.2$ Hz; H-2'); 5.29 (br s; 1H; 4'-OHg); 5.39 (m; 1H; H-4'); 5.79 (dt; 1H; $J = 10.3$ Hz; $J = 2.3$ Hz; H-3); 6.13 (dd; 1H; $J = 10.3$ Hz; $J = 1.1$ Hz; H-2); 6.38, 6.42 (2 × d; 2H; $J = 2.4$ Hz; H-6g, H-8g); 6.91 (d; 2H; $J = 8.8$ Hz; H-3'g; H-5'g); 7.41 (d; 2H; $J = 8.8$ Hz; H-2'g, H-6'g); 7.86 (s; 1H; H-2g); 12.82 (s; 1H; 5g-OH). LRMS (ESI) Calcd $C_{39}H_{42}O_{19}$ [M+Na]⁺ 837.2218. Found 837.4.

5-Hydroksy-7-[(4-O-(2,3,4,6-tetra-O-acetyl- β -D-galactopyranosyl)-6-O-acetyl-2,3-dideoxy- α -D-erythro-hex-2-enopyranosyl)-3-O-propyl]-3-(4-hydroksyphenyl)chromen-4-one (9b). Obtained after chromatography as colorless syrup, in 78% yield; ¹H NMR (CDCl₃) δ : 1.98 (s; 3H; AcO); 2.05 (s; 3H; AcO); 2.07 (s; 3H; AcO); 2.11 (s; 3H; AcO); 2.15 (s; 3H; AcO); 2.07–2.13 (m; 2H; -CH₂-); 3.66

(dt; 1H; $J = 9.9$ Hz; $J = 6.2$ Hz; -CH₂O-); 3.91–3.95 (m; 2H; H-5', -CH₂O-); 3.99 (ddd; 1H; $J = 1.9$ Hz, $J = 5.4$ Hz, $J = 9.5$ Hz, H-5); 4.09–4.27 (m; 7H; H-4, H-6a, H-6b, H-6a', H-6b'; -CH₂O-); 4.57 (d; 1H; $J = 7.9$ Hz; H-1'); 5.00 (br s; 1H; H-1); 5.00 (dd; 1H; $J = 10.4$ Hz; $J = 3.5$ Hz; H-3'); 5.20 (dd; 1H; $J = 10.4$ Hz; $J = 7.9$ Hz; H-2'); 5.38 (dd; 1H; $J = 3.5$ Hz; $J = 1.0$ Hz; H-4'); 5.61 (br s; 1H; 4'-OHg); 5.75 (ddd; 1H; $J = 10.4$ Hz; $J = 2.8$ Hz; $J = 2.2$ Hz; H-3); 6.12 (dd; 1H; $J = 10.4$ Hz; H-2); 6.36, 6.40 (2 × d; 2H; $J = 2.4$ Hz; H-6g, H-8g); 6.89 (d; 2H; $J = 8.6$ Hz; H-3'g; H-5'g); 7.39 (d; 2H; $J = 8.6$ Hz; H-2'g, H-6'g); 7.86 (s; 1H; H-2g); 12.80 (s; 1H; 5g-OH). LRMS (ESI) Calcd $C_{40}H_{44}O_{19}$ [M+Na]⁺ 851.2374. Found 851.4.

5-Hydroksy-7-[(4-O-(2,3,4,6-tetra-O-acetyl- β -D-galactopyranosyl)-6-O-acetyl-2,3-dideoxy- α -D-erythro-hex-2-enopyranosyl)-5-O-pentyl]-3-(4-hydroksyphenyl)chromen-4-one (9d). Obtained after chromatography as colorless syrup, in 53% yield; ¹H NMR (CDCl₃) δ : 1.49–1.58 (m; 2H; -CH₂-); 1.63–1.70 (m; 2H; -CH₂-); 1.77–1.88 (m; 2H; -CH₂-); 1.98 (s; 3H; AcO); 2.05 (s; 3H; AcO); 2.08 (s; 3H; AcO); 2.12 (s; 3H; AcO); 2.16 (s; 3H; AcO); 3.51 (dt; 1H; $J = 9.5$ Hz; $J = 6.3$ Hz; CH₂O); 3.66 (m; 1H; H-5'); 3.79 (dt; 1H; $J = 9.5$ Hz; $J = 6.3$ Hz; CH₂O); 3.87–4.23 (m; 8H; H-5, -CH₂O-, H-6a, H-6b, H-6a', H-6b', H-4); 4.58 (d; 1H; $J = 8.1$ Hz; H-1'); 4.96–5.03 (m; 2H; H-1; H-3'); 5.22 (dd; 1H; $J = 10.3$ Hz, $J = 8.1$ Hz; H-2'); 5.39 (dd; 1H; $J = 3.7$ Hz; $J = 1.0$ Hz; H-4'); 5.77 (ddd; 1H; $J = 10.3$ Hz; $J = 2.2$ Hz; $J = 2.5$ Hz; H-3); 6.09–6.13 (m; 2H; H-2; 4'-OHg); 6.35, 6.38 (2 × d; 2H; $J = 2.2$ Hz; H-6g; H-8g); 6.88 (d; 2H; $J = 8.7$ Hz; H-3'g, H-5'g); 7.37 (d; 2H; $J = 8.7$ Hz; H-2'g, H-6'g); 7.85 (s; 1H; H-2g); 12.81 (s; 1H; 5g-OH). LRMS (ESI) Calcd $C_{42}H_{48}O_{19}$ [M+Na]⁺ 879.2686. Found 879.4.

2.1.2.4. Procedure for synthesis of *n*-propyl-2,3-unsaturated pyranoside (10).

To a solution of rhamnal (5) (0.2 mM) in anhydrous dichloromethane (40 mL) 1-propanol (0.2 mM) and BF₃·Et₂O (0.02 mM) was added. The contents were stirred at temperature -25 °C to 10 °C for 0.5 h and the reaction monitored by TLC (toluene/AcOEt = 1:1 (v/v)). The reaction mixture was quenched by the addition of aqueous sodium hydrogen carbonate (10%, 25 mL), extracted with dichloromethane (3 × 25 mL), dried over anhydrous sodium sulfate, filtered and washed with water, and the combined organic extract was concentrated under vacuum. The residue was purified by column chromatography (90:1 petroleum ether/AcOEt) on silica gel to obtain the product 10 as colorless syrup, in 50% yield.

Propyl 4-O-acetyl-2,3,6-trideoxy- α -L-erythro-heks-2-en-pyranoside (10). ¹H NMR (CDCl₃) δ : 0.95 (t; 3H; $J = 7.3$ Hz; -CH₃); 1.22 (d; 3H; $J = 6.3$ Hz; H-6); 1.59–1.74 (m; 2H; -CH₂-); 2.08 (s; 3H; AcO); 3.46 (dt; 1H; $J = 9.5$ Hz; -CH₂O-); 3.72 (dt; 1H; $J = 9.5$ Hz -CH₂O-); 3.98 (dq; 1H; $J = 9.2$ Hz, $J = 6.3$ Hz; H-5); 4.96 (br s; 1H; H-1); 5.05 (dd; 1H; $J = 9.2$ Hz; H-4); 5.81 (ddd; 1H; $J = 10.3$ Hz; H-3); 5.84 (d; 1H; $J = 10.3$ Hz; H-2).

2.2. Biological activity

2.2.1. Cells

Human, A-549 (lung), LNCaP, DU145 and PC3 (prostate), MCF-7 and SKBR-3 (breast), HCT116, HT-29, LOVO and Caco-2 (colon), AGS (stomach) cancer and T98G (glioblastoma) cell lines were obtained from American Type Culture Collection (Rockville, Maryland, USA). A-549, LNCaP, MCF-7, SKBR-3, HT-29 cancer and T98G cell lines are being maintained in the Institute of Immunology and Experimental Therapy, Wrocław, Poland. DU145, PC3, LOVO, Caco-2 and AGS cell lines are being maintained in Maria Skłodowska-Curie Memorial Cancer Center and the Institute of Oncology, Gliwice, Poland.

LNCaP and HT-29 cells were cultured in RPMI 1640+Opti-MEM (1:1) medium (Gibco, Scotland, UK) supplemented with 2 mM L-glutamine, 1 mM sodium pyruvate and 5% fetal bovine serum (all from Sigma-Aldrich Chemie GmbH, Steinheim, Germany).

A-549 cells in RPMI 1640+Opti-MEM (1:1) medium (both from Gibco, Scotland, UK) supplemented with 2 mM L-glutamine and 5% fetal bovine serum (all from Sigma–Aldrich Chemie GmbH, Steinheim, Germany). MCF-7 and SKBR-3 cells in Eagle medium (IJET, Wrocław, Poland) supplemented with 2 mM L-glutamine, 1.0 mM sodium pyruvate, 1% amino acid, 0.8 mg/L of insulin and 10% fetal bovine serum (all from Sigma–Aldrich Chemie GmbH, Steinheim, Germany). T98G cells in Eagle medium (IJET, Wrocław, Poland) supplemented with 2 mM L-glutamine, 1.0 mM sodium pyruvate, 1% amino acid and 10% fetal bovine serum (all from Sigma–Aldrich Chemie GmbH, Steinheim, Germany). DU145, PC3, LOVO, Caco-2, AGS cells were cultured in RPMI 1640 medium (Sigma–Aldrich, Germany) supplemented with 10% fetal bovine serum (MP Biomedicals, LLC). HCT116 cells were cultured McCoy's 5A medium (Sigma–Aldrich, Germany) supplemented with 10% fetal bovine serum (MP Biomedicals, LLC, United States).

All culture media were supplemented with 100 units/mL penicillin, and 100 µg/mL streptomycin (both from Polfa Tarchomin S.A., Warsaw, Poland) and all cell lines were grown at 37 °C with 5% CO₂ humidified atmosphere.

2.2.2. Cytotoxicity assays

Cell viability was estimated using an MTT (3-[4,5-dimethylthiazol-2-yl]2,5-diphenyltetrazolium bromide) assay (Sigma–Aldrich, Germany), according to the supplier's protocol or SRB (sulforhodamine B) assay. Shortly, 24 h before addition of the tested compounds, the cells were plated in 96-well plates (Sarstedt, Germany) at the density of 2×10^3 cells per well. Assays were performed after 72 h of continuous exposure to varying concentrations of the tested agents. Each compound in each concentration was tested in triplicate in a single experiment, which was repeated at least three times. Viability of cells was expressed as a percentage versus vehicle control (DMSO treatment). IC₅₀ was defined as a concentration of a drug that decreased cell viability by 50%.

2.2.3. MTT assay

After 72 h treatment with tested agents the medium was aspirated and cells were incubated for 3 h at 37 °C with 0.5 mg/mL MTT solution (50 µL) in Dulbecco modified essential medium (DMEM) (Sigma–Aldrich, Germany) without phenol red. Then the medium was aspirated, insoluble crystals of formazan were solubilized in 2-propanol/HCl solution, and optical density ($\lambda = 570$ nm) was determined in a microplate reader BioTek Synergy II (BioTek Instruments, USA).

2.2.4. SRB assay

The cells were attached to the bottom of plastic wells by fixing them with cold 50% TCA (trichloroacetic acid, Sigma–Aldrich Chemie GmbH, Steinheim, Germany) on the top of the culture medium in each well. The plates were incubated at 4 °C for 1 h and then washed five times with tap water. The cellular material fixed with TCA was stained with 0.4% sulforhodamine B (SRB, Sigma–Aldrich Chemie GmbH, Steinheim, Germany) dissolved in 1% acetic acid (POCH, Gliwice, Poland) for 30 min. Unbound dye was removed by rinsing (4×) in 1% acetic acid. The protein-bound dye was extracted with 10 mM unbuffered Tris base (Sigma–Aldrich Chemie GmbH, Steinheim, Germany) for determination of the optical density ($\lambda = 540$ nm) in a microplate reader Multiskan RC photometer (Labsystems, Helsinki, Finland).

2.2.5. Cell cycle analysis

Cells in subconfluent proliferating cultures were incubated with the tested compounds continuously for indicated period of time. Floating cells were collected and added to adherent cells, harvested by trypsinization. Cells were washed with PBS and then fixed in ice-cold ethanol (70%) for 30 min, treated with RNase (100 µg/mL) and

stained with propidium iodide (PI) (100 µg/mL). The DNA content was analyzed using Becton Dickinson FACSCanto cytometer (BD Company, USA) to monitor the cell cycle changes. Experiments were repeated at least twice.

2.2.6. Mitotic index

Cells, collected as described above, were cytospinned, fixed with cold methanol, stained with solution of DAPI (3 µM). Slides were mounted in DAKO® Fluorescent Mounting Medium (Dako, USA) and examined under an ECLIPSE E800 Nikon microscope using an objective 40×. Mitotic cells were counted among 1000 cells. Experiments were repeated three times.

2.2.7. Tubulin immunostaining

Cells growing on 8-well chamber slides (Lab-Tek Permanox® slides, Nalgen Nunc International, Rochester, NY, USA) were treated with the tested compounds for 24 h. Cells were fixed in ice-cold methanol (–20 °C) for 10 min, air-dried, immediately washed in PBS and blocked with normal goat serum (NGS) (1%; Vector Laboratories, Burlingame, CA, USA) for 0.5 h in a humidified chamber at room temperature. Then, the slides were treated for one hour with mouse anti-β-tubulin (1:50, v/v; Sigma–Aldrich, Germany). After subsequent three rinses in PBS, cells were incubated for 0.5 h with goat anti-mouse FITC-conjugated secondary antibody (Sigma–Aldrich, Germany), rinsed several times in PBS, and counterstained with solution of DAPI (3 µM). Slides were mounted in DAKO® Fluorescent Mounting Medium (Dako, USA).

2.2.8. Analysis of spindle abnormalities

Ram-3 treated cells immunofluorescently stained for tubulin were examined under the ECLIPSE E800 Nikon microscope using an oil immersion objective 100×. For each treatment 100 of mitotic cells were analyzed for abnormalities. Experiments were repeated twice. Photographs of representative spindles were taken with Hamamatsu C5810 camera (Hamamatsu Photonics, Japan).

2.2.9. In vitro tubulin polymerization assay

The effects of **Ram-3** on tubulin polymerization were investigated using the HTS-Tubulin Polymerization Assay Kit CytoDYNA-MIX Screen™ 1 (CDS01, Cytoskeleton Inc. Denver, CO, USA), according to the manufacturer protocol. Tubulin dimers (>97% purity) were suspended with 100 µL of G-PEM buffer (80 mM PIPES, 2 mM MgCl₂, 0.5 mM EGTA, 1 mM GTP, pH 6.9) plus 5% glycerol. Tests were run in the absence (vehicle control used as a reference) or presence of the test compounds (10 µM, 20 µM and 50 µM **Ram-3** and 3 µM paclitaxel) in pre-warmed (37 °C) 96-well plate. The polymerization of tubulin was followed by measuring the increase in absorbance at 340 nm as a function of time (every minute for 1 h) at 37 °C. The experiments were repeated twice.

2.2.10. Apoptosis detection

2.2.10.1. Agarose gel electrophoresis/DNA ladder analysis. Cells treated with **Ram-3** or untreated control were collected and washed with PBS. Cells were incubated overnight at 56 °C with 50 mM Tris (pH 7.5), 100 mM EDTA, 1% SDS, 150 mM NaCl, 1 mg/mL proteinase K, and next treated with phenol/ chloroform to extract DNA. DNA was precipitated with isopropanol/sodium acetate, treated with 0.1 mg/mL RNaseA, and then separated in a 1.8% agarose/ethidium bromide gel in 0.5×TBE (90 mM Tris, 64.6 mM boric acid, 2.5 mM EDTA, pH 8.3). After electrophoresis DNA was visualized by UV light and photographed.

2.2.10.2. Terminal deoxynucleotidyl transferase dUTP nick-end labeling (TUNEL assay). TUNEL assay was performed according to a manufacturer protocol (ROCHE) with slight modifications. In brief, floating cells were harvested and pooled with adherent cells

detached from the bottom of a culture dish by trypsin. Cells were cytospinned, fixed and then the slides were treated following the section of a protocol for adherent cells. Apoptotic index was counted in 500 nuclei. Experiments were repeated three times.

2.2.11. Cell senescence analysis

Morphological features of cells, such as cell size increase and accumulation of intracellular vesicles were observed under phase contrast microscope. Senescence-associated- β -galactosidase (β -gal) activity was chosen as a biochemical marker for replicative senescence.¹⁹ In order to show β -gal activity cells were fixed for 5–10 min in 4% paraformaldehyde, washed and incubated with fresh staining solution (1 mg/mL of X-gal diluted in the staining buffer [40 mM citric acid/sodium phosphate pH6.0, 5 mM potassium ferrocyanide, 5 mM potassium ferricyanide, 150 mM NaCl, 2 mM MgCl₂]) for 12 h at 37 °C.

3. Results and discussion

3.1. Chemistry

The synthesis of required compounds, designed through inspiration with unusual biological activity of unsaturated genistein glycoside G21,⁸ was accomplished according to general pathway illustrated in Figures 1–3. Compounds **3a**, **3b**, **3d** were the key intermediates for the synthesis of the glycoconjugates.

In the first step, genistein was converted into an intermediate bearing an ω -hydroxyalkyl substituent, containing two, three or five carbon atoms, at position 7, while the second step involved glycosylation. Genistein quaternary ammonium salts (**2**) were applied to complete the alkylation step. Resulting compounds (**3a**, **3b**, **3d**), which contain aliphatic primary hydroxyl functionality, easily react with acylated glycals (hex-1-enitols) under Lewis acid catalysis, undergoing Ferrier rearrangement. The reaction is highly regio- and stereo-selective, affording glycosides with α -configuration. Both synthetic steps are in principle very simple, but deserve some comments, when applied to a multifunctional substrate like genistein (**1**).

Several procedures are known, which were successfully applied for alkylation of genistein.

Thus, regioselective alkylation of genistein was performed by treatment of genistein with haloalkanes in the presence of base like NaOH, K₂CO₃ in anhydrous acetone.^{20,21} Bromoalkyl derivatives of genistein were obtained in reaction of **1** with 1,2- 1,3- or 1,4-dihaloalkanes under ultrasound irradiation.²²

However, in our hands, reaction of genistein (**1**) with 3-bromopropanol invariably afforded a mixture of 7-*O* and 4'-*O*-hydroxyalkyl ethers, which are difficult to separate. In contrast,

similar alkylation performed on well defined tetra-*n*-butylammonium salt of genistein (**2**),²³ proceeded smoothly even with equimolar amount of 3-bromopropanol (and 2-bromoethanol), affording required product with very high regioselectivity. Synthesis of 5-hydroxypentyl derivative by the same procedure has failed, because the substrate was consumed by competing intramolecular cyclization reaction, which produced tetrahydrofuran. In this case, 5-bromopentyl acetate was used as alkylating reagent and subsequently the hydroxyl group was liberated through methanolysis.

The Lewis acid-catalyzed allylic rearrangement of glycals in the presence of alcohols and other nucleophilic substrates (phenols) is the method of choice for the synthesis of 2,3-unsaturated glycosides. The reaction, as originally stated by Ferrier, involves intermediacy of a cyclic allylic oxocarbenium ion to which the nucleophile adds preferentially in quasi-axial orientation. Typically, 2,3-unsaturated *O*-glycosides are prepared by Ferrier rearrangement of acyloxy glycals catalyzed by boron trifluoride diethyl etherate.^{24–27}

Owing to its significance in carbohydrate and natural product chemistry, there has been a growing interest in identifying new catalysts for the Ferrier reaction. The use of a number of reagents for this transformation has appeared in the recent literature, including titanium(IV) chloride (TiCl₄),²⁸ indium(III) chloride (InCl₃),^{29,30} indium(III) bromide (InBr₃),³¹ acidic montmorillonite K-10,^{32–34} tin(IV) chloride (SnCl₄).^{35,36}

The efficacy of selected catalysts: boron trifluoride etherate (BF₃·Et₂O), ytterbium(III) triflate (Yb(OTf)₃), indium(III) chloride (InCl₃) was examined for the Ferrier rearrangement of **3b** in reaction with **5**. In the presence of BF₃·Et₂O an equimolar mixture of α , β -glycosides was formed. The ytterbium(III) triflate was inactive under our conditions. It was observed, that among mentioned catalysts, InCl₃ is superior in terms of the stereoselectivity and yield. Thus, in the presence of InCl₃ and acetonitrile as a solvent the reaction of **3b** with **5** proceeds at ambient temperature and millimolar scale glycosylation is completed within less than 2 h, with equimolar proportion of nucleophile, to give good yield of α -*O*-glycoside. Glycosylation of remaining hydroxyalkyl-genistein derivatives with glycals was performed under analogous conditions.

3.2. Biological activity

3.2.1. Preliminary screening of the compounds for antiproliferative activity and their influence on the cell cycle

Preliminary screening of new compounds for their antiproliferative activity was performed in a standard 72 h MTT assay on HCT116 cell line. The data expressed as the concentration leading to 50% inhibition of cell viability (IC₅₀), for each genistein derivative is summarized in Table 1. It can be seen that the derivatives named **Gen-5**, **Glu-5**, **Ram-2**, **Ram-3** and **Ram-5**, exhibited cytotoxic effect

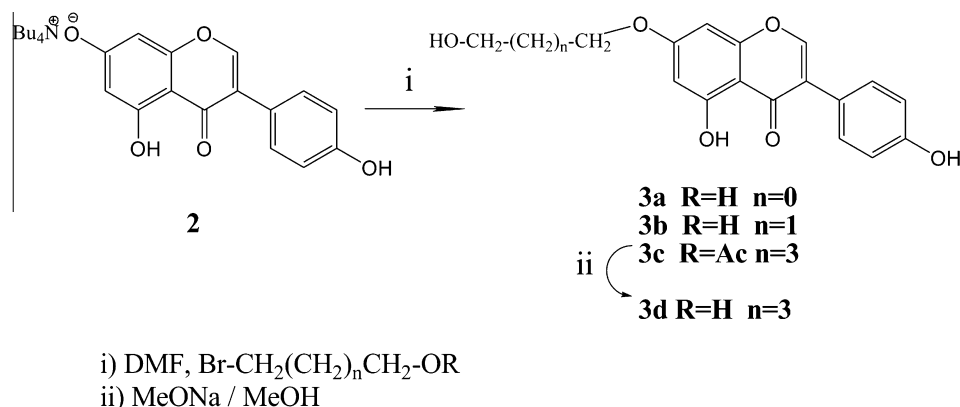


Figure 1. Synthesis of hydroxyalkyl-genistein derivatives.

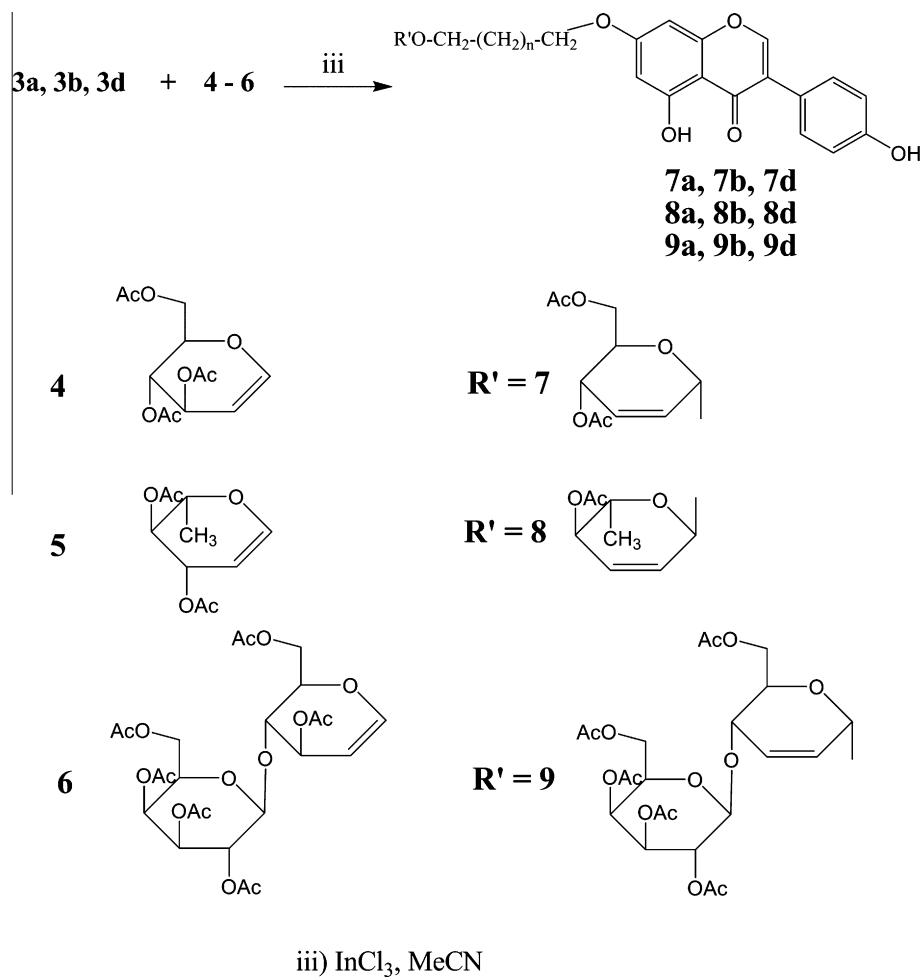


Figure 2. Synthesis of glycoconjugates, derivatives of genistein.

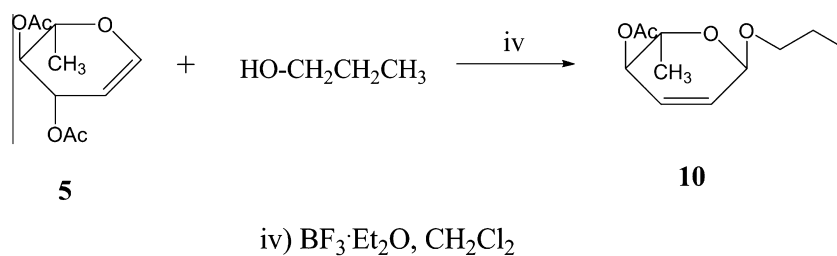


Figure 3. Synthesis of propyl glycoconjugate.

at the concentration significantly lower (IC₅₀ below 10 μM), as compared to genistein (IC₅₀ approx. 35 μM). Cytotoxic assays revealed that the sugar moiety was not toxic (Table 1). Also, the treatment of cells with a combination of genistein and rhamnal derivative did not evoke any synergistic effect (data not shown).

Five compounds: **Gen-5**, **Glu-5**, **Ram-2**, **Ram-3** and **Ram-5** showing highest activity in MTT assay were selected for further analysis of cell cycle and determination of apoptosis with flow cytometer.

Flow cytometry analysis in PI stained cells shown the occurrence of apoptotic cells, after treatment with genistein **Gen-5** and **Glu-5**, seen on the histograms as a population on the left from the G₁ peak (Fig. 4). The analysis of histograms revealed also the influence of genistein and some of derivatives on the cell cycle (Fig. 4). In control cells (the first histogram in each set, marked

as 0 μM) roughly 50% of cells were in G₁ phase of a cycle (high G₁ peak), and around 24% of cells were in G₂ or M phase (low G₂/M peak). After genistein treatment the shift of cells from G₁ to G₂/M phase can be seen. Dose-dependent increase of cells arrested in the G₂/M was also observed after treatment of HCT116 cells with **Glu-5**, **Ram-3** and **Ram-5**, with the most prominent effect observed after treatment with **Ram-3**. Neither **Ram-2** nor **Gen-5** influenced the cell cycle.

3.2.2. The effect of genistein derivatives on mitosis

In order to find whether a G₂/M block of a cycle results from arresting cells in G₂ phase or in mitosis, we counted the mitotic index in cells treated for 24 h with 20 μM of **Gen-5**, **Glu-5**, **Ram-2**, **Ram-3** and **Ram-5** and genistein (Table 2). Additionally, bearing in mind that 20 μM concentration of the tested derivatives exceeds

Table 1

Comparison of cytotoxicity of new compounds in HCT116 colon cancer cell line

Tested compound	IC ₅₀ ^a (μM)
Genistein (1)	34.90 ± 9.84
Gen-2 (3a)	24.99 ± 12.07
Gen-3 (3b)	23.93 ± 3.90
Gen-5 (3d)	6.92 ± 2.06
Lac-2 (2a)	>20 ^b
Lac-3 (9a)	>20 ^b
Lac-5 (9a)	>20 ^b
Glu-2 (9d)	16.06 ± 7.26
Glu-3 (7b)	19.86 ± 6.01
Glu-5 (7d)	8.45 ± 1.74
Ram-2 (8a)	9.32 ± 3.44
Ram-3 (8b)	4.76 ± 0.96
Ram-5 (8d)	8.08 ± 2.97
Ram-P (10)	550 ± 11.08

^a Concentration of a tested compound leading to 50% inhibition of cell proliferation (IC₅₀) was obtained in a standard 72 h MTT assay; mean values and standard deviations were calculated from at least three independent experiments.

^b Cytotoxicity was not assessed above the concentration 20 μM due to low substance solubility and its precipitation.

their IC₅₀ at least twice, we used a 100 μM genistein. It can be seen that three genistein derivatives (**Glu-5**, **Ram-3**, **Ram-5**), but not genistein, blocked cells in mitosis, with the most profound effect observed for **Ram-3**. However, the subtraction of mitotic index from the fraction of cells stopped in G₂/M phase in flow cytometry analysis showed that all three compounds substantially blocked cell cycle not only in mitosis but also in G₂ phase. In contrast, genistein used at high concentration (100 μM) caused cells to stop entering the mitosis, and mitotic index dropped rapidly.

In our previous paper we found that the unsaturated genistein disaccharide glycoside G21 blocked cells in mitosis due to induction of abnormal mitotic spindles,⁷ and the data presented above suggested that **Ram-3** (and two other compounds **Glu-5** and **Ram-5** to a lower extent) could exhibit the same mode of action. The analysis of **Ram-3** treated HCT116 cells shown various abnormalities of the mitotic spindles, including multipolarity and lagging chromosomes at the spindle poles (Fig. 5). Frequency of abnormal spindles was dose-dependent (Table 3), exceeding 80% after treatment with 20 μM **Ram-3**. We also analyzed cells after treatment with 20 μM and 50 μM **Ram-3** for any changes of interphase microtubule array. At 20 μM **Ram-3** we observed no alteration, but at 50 μM (the concentration ten times exceeding IC₅₀), less dense and shortened microtubules were visible (not shown). The difference between the concentration at which spindles were affected and the concentration at which changes to interphase array occurred is not unusual, as it is well recognized that microtubule binding agents cause perturbations to mitotic spindles at much lower concentration, than, when used for microtubule depolymerization.^{37,38} The differences between dynamics of interphase and mitotic spindle microtubules, correlating with different sensitivity of those arrays to microtubule binding drugs are well described phenomena. During mitosis microtubules show highly dynamic instability, which is necessary for proper function of a spindle, and any disturbance of this instability blocks the progression of mitosis from metaphase to anaphase without net depolymerization of microtubules.^{39–42}

Although multiple molecular targets for antimetabolic drugs are known, including tubulins and various mitotic kinases, all of them, either by interfering with the proper attachment of chromosomes to the microtubules of mitotic spindle or altering the structure of a

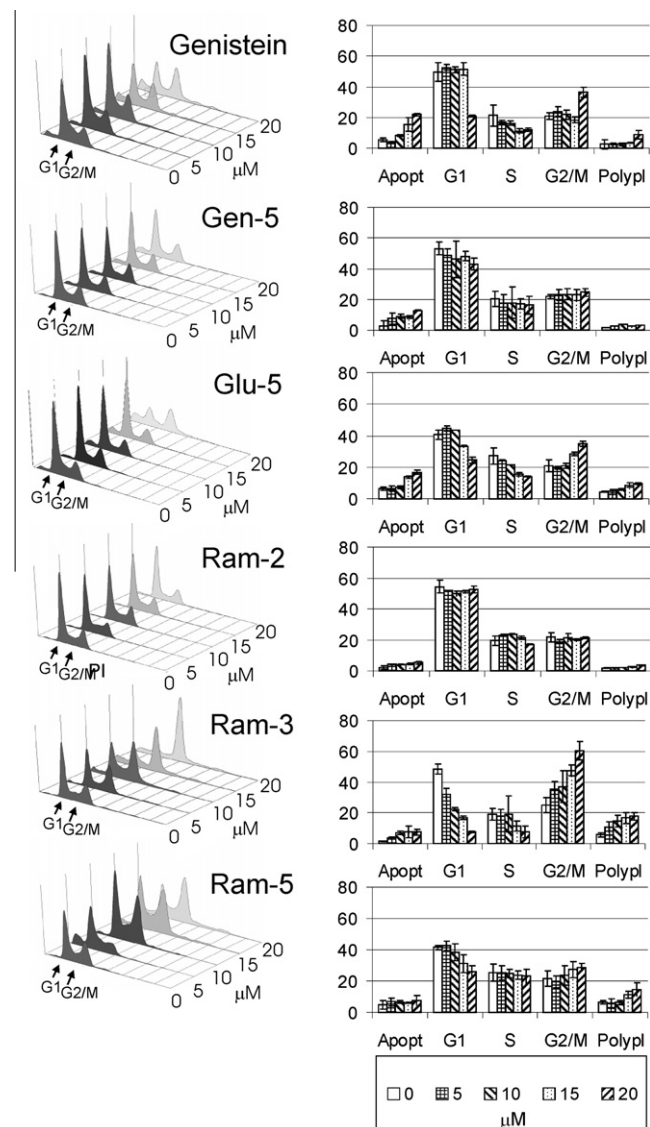


Figure 4. Cell cycle phases distribution in HCT116 cells treated with different genistein derivatives at growing concentration series for 24 h. Left—representative histograms of cells with different DNA contents. G1—cells in G1 phase of a cycle; G2/M—cells in G2 phase of a cycle or in mitosis. Right—mean values and standard deviations from independent experiments. Apopt—apoptotic cells; G1—cells in G1 phase; S—cells in the S phase; G2—cells in G2 or M phase; Polypl—polyploid cells.

Table 2

Mitotic index in HCT116 cells treated with different genistein derivatives for 24 h

Treatment	Mitotic index at 24 h treatment ^a
Control	1.9 ± 0.6
Genistein [20 μM; 100 μM]	1.8 ± 0.4; 0.5 ± 0.2
Gen-5 [20 μM]	3 ± 1.6
Glu-5 [20 μM]	5.2 ± 0.9
Ram-2 [20 μM]	1.3 ± 0.2
Ram-3 [20 μM]	13.2 ± 2.1
Ram-5 [20 μM]	3.5 ± 1.1

^a Mean values and standard deviation were obtained from three independent experiments. Mitotic index was counted in 1000 nuclei in each treatment.

spindle (i.e., change of the number of spindle poles), induce mitotic checkpoint arrest of a cell cycle.^{43,44}

In order to determine whether **Ram-3** can directly interact with microtubules, we performed microtubule polymerization in

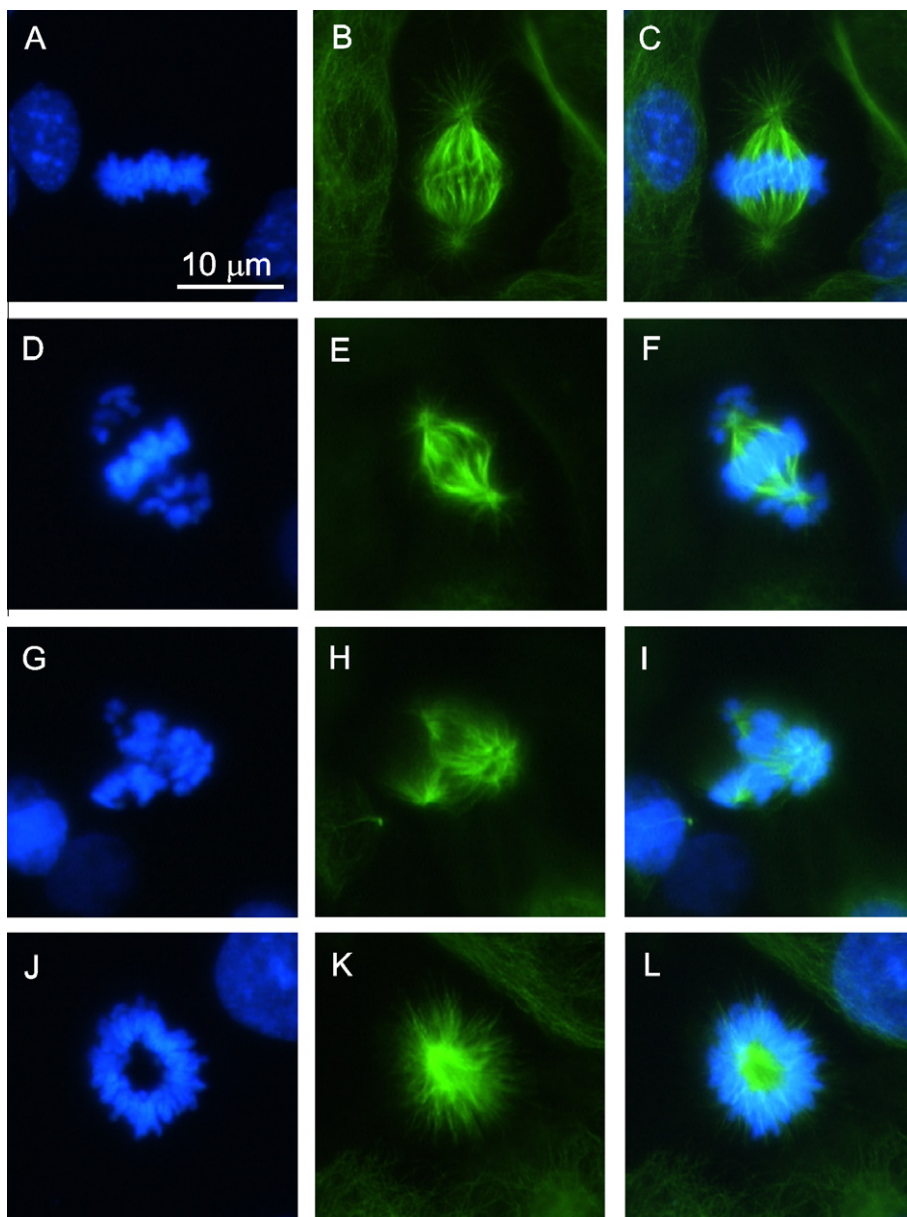


Figure 5. Spindle structure in **Ram-3** treated HCT 116 cells. (A–C) Normal bipolar spindle (Type a); (D, E) bipolar spindle with large masses of lagging chromosomes at spindle poles (Type b); (G–I) Tripolar spindle (Type c); (J–L) monopolar spindles (Type d).

Table 3
Spindle abnormalities in HCT116 cells after treatment with **Ram-3** for 24 h

Ram-3 (μM)	Normal spindles	Aberrant spindles			Total (%)
	Type a ^a (%)	Type b ^b (%)	Type c ^c (%)	Type d ^d (%)	
0	94 \pm 3	1 \pm 0	5 \pm 3	0 \pm 0	6 \pm 3
5	85 \pm 6	14 \pm 6	1 \pm 0	0 \pm 0	15 \pm 6
10	44 \pm 8	38 \pm 7	15 \pm 3	3 \pm 1	56 \pm 8
20	16 \pm 3	40 \pm 7	42 \pm 6	2 \pm 1	84 \pm 3

^a Type a—normal bipolar spindle.

^b Type b—bipolar spindle with large mass of lagging chromosomes at spindle poles.

^c Type c—tripolar and multipolar spindles.

^d Type d—monopolar spindles. Aberrant spindles were counted among 100 mitotic cells in each treatment. Mean values and standard deviations were obtained from two independent experiments.

cell-free system, using a standard assay (Fig. 6). In the presence of paclitaxel (3 μM), the agent stimulating tubulin polymerization,

the rate of tubulin polymerization increased dramatically as compared to the control, whereas **Ram-3** inhibited tubulin

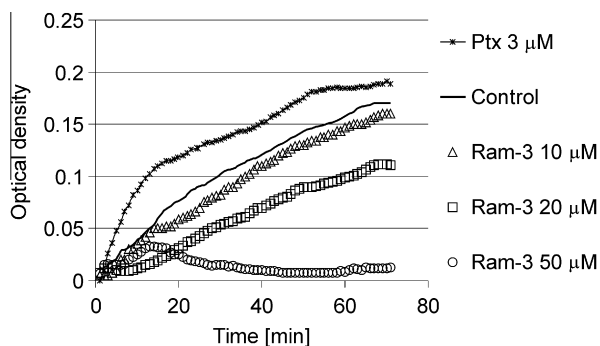


Figure 6. Tubulin polymerization assay in cell-free system. Optical density of tubulin solution measured spectrophotometrically at 340 nm in the absence of drugs (control) or in the presence of 3 μM paclitaxel (Ptx) and 10 μM , 20 μM and 50 μM of **Ram-3**.

polymerization in a concentration dependent manner. This result indicates, that **Ram-3** can be classified as a new microtubule destabilizing agent.

3.2.3. Cell death and senescence after **Ram-3** treatment

Cell cycle arrest in mitosis strongly influences the fate of cells treated with antimetabolic drugs and loss of their proliferative potential. Usually, cells are not able to sustain prolonged mitotic arrest and eventually escape from the mitosis, which is called mitotic slippage. In this process cells decondense the chromatin, but incomplete or improper division in many cases leads to tetraploidy, often followed by cell death.^{45,46} The decrease of mitotic index from 13% after first day of treatment to 6% and 4% after the second and third day of treatment, respectively indicates that cells, initially blocked in mitosis by **Ram-3** treatment, could gradually escape from the block within the period of few days following mitotic arrest. Morphological observations during second and third day of treatment shown many rounded cells, with membrane blebbings (data not shown), suggesting massive apoptotic cell death. Flow cytometry analysis revealed the presence of increased fraction of both hypodiploid and tetraploid populations after 48 and 72 h of treatment (Fig. 7). Apoptotic death, suggested by

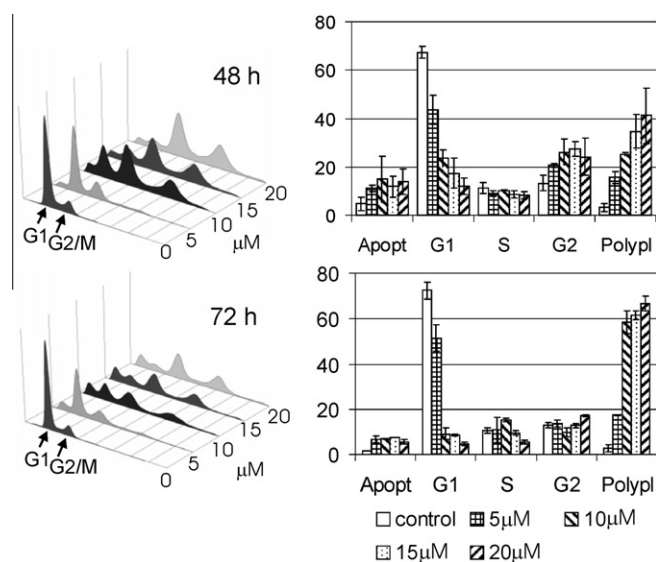


Figure 7. DNA content in HCT116 cells treated with **Ram-3** for 48 and 72 h. Left—representative histograms of cells with different DNA contents. G_1 —cells in G_1 phase of a cycle; G_2/M —cells in G_2 phase of a cycle or in mitosis. Right—mean values and standard deviations from independent experiments. Apopt—apoptotic cells; G_1 —cells in G_1 phase; S—cells in the S phase; G_2 —cells in G_2 or M phase; Polypl—polypliod cells.

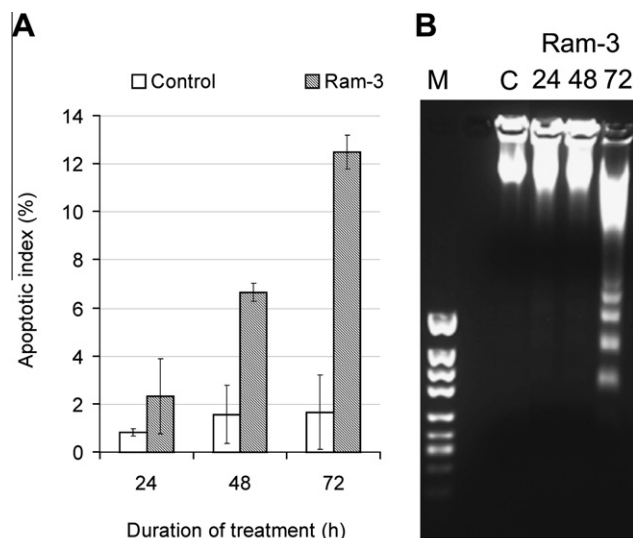


Figure 8. Apoptotic events after 24, 48, 72 h treatment of HCT116 cells with 20 μM **Ram-3**. Control cells treated with 0.2% DMSO in culture medium. (A) Index of TUNEL positive nuclei (apoptotic index) counted in 500 nuclei. Mean value and standard deviation obtained from three independent experiments. (B) Internucleosomal DNA fragmentation (DNA laddering). Lane 1 (M)—marker; lane 2 (C)—control cells; lanes 3–5 (**Ram-3** 24, 48, 72 h) cells treated with **Ram-3** for indicated time.

morphological features and hypodiploidy was confirmed by TUNEL assay and by internucleosomal DNA fragmentation (Fig. 8). The apoptotic index calculated for cells exposed to **Ram-3** for 72 h reached 12%, what roughly corresponded to the intensity of the mitotic block observed after 24 h treatment.

Ram-3 treatment led to elimination of substantial fraction of HCT116 cells by apoptosis on one hand, and to the loss of the proliferative potential of remaining cells on the other. Increase of tetraploid and polyploid cells fraction after 48 h and 72 h of treatment was accompanied by the decrease of the mitotic index, and the presence of cells with senescent phenotype (Fig. 9). Many cells were enlarged, and shown positive perinuclear staining of the sites of β -galactosidase activity ($31 \pm 4\%$).

It is known that mitotic slippage activates checkpoint machinery in tetraploidized cells, which inhibits progression of the cell cycle at G_1 and phase, dependent on the tumor suppressor protein p53.⁴⁷ Thus we decided to compare the rate of apoptotic cell death in two isogenic HCT116 cell lines, differing their p53 status: HCT116 p53 $^{-/-}$ and HCT116 p53 $^{+/+}$. In general, the cytotoxicity of **Ram-3** against two lines was similar, and IC_{50} was $6.21 \pm 1.13 \mu\text{M}$ and $4.76 \pm 0.96 \mu\text{M}$, respectively. The similar apoptotic index (15% for p53 $^{-/-}$ and 12% for p53 $^{+/+}$) indicates that HCT116 cells treated with **Ram-3** may enter apoptosis regardless of the p53 status.

3.2.4. Antiproliferative activity of **Ram-3** against cancer cell lines of different origin

Antiproliferative potential of **Ram-3** and genistein was assessed in additional 11 human cell lines of different origin: glioblastoma, breast, colon, prostate, lung and stomach cancers (Table 4). In all tested lines we observed stronger inhibition of cell growth by **Ram-3** than by genistein. The susceptibility of different cell lines to **Ram-3** differed to some extent, but we did not observe any organ specific activity of **Ram-3**. We also tested the influence of **Ram-3** on the cell cycle in three cell lines, in addition to HCT116: AGS, A549 and DU145, observing cell cycle arrest in G_2/M phase. In selected cell lines the fraction of cells in G_2/M before and after treatment with 20 μM **Ram-3** increased: in AGS cell

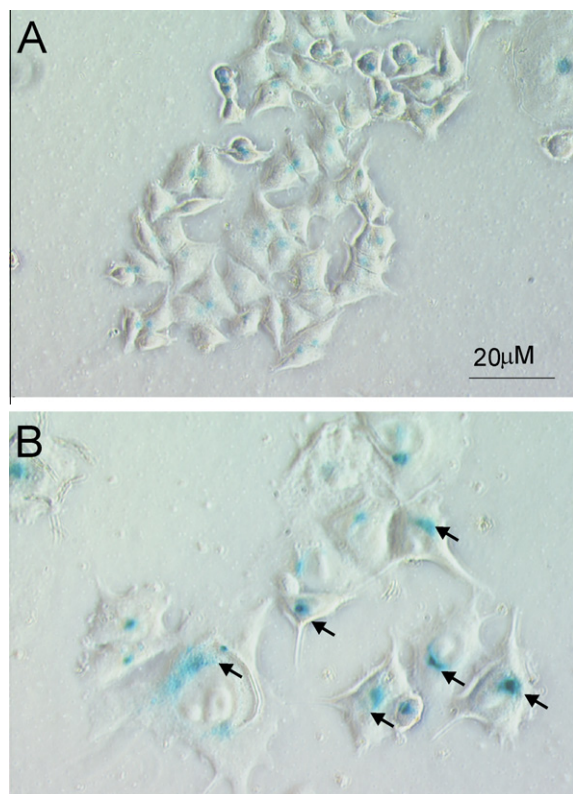


Figure 9. Senescent phenotype of HCT116 cells after 24 h treatment with **Ram-3**. Arrows indicate enlarged cells with blue, perinuclear staining of the sites of β -galactosidase activity.

line—from $24.3 \pm 0.2\%$ to $39.7 \pm 2.2\%$, in A549—from $21.9 \pm 3\%$ to $31.6 \pm 4.9\%$ and in Du145—from $27.6 \pm 0.1\%$ to $46.1 \pm 8\%$.

3.2.5. Relevance of structural features of glycoconjugates for their biological activity

Data obtained so far neither allow to depict a single parameter which could determine structure–activity relationship, nor unequivocally indicate molecular targets of genistein glycoconjugates responsible for their antiproliferative and antimetabolic activity.

The increase of antiproliferative potential of genistein derivatives with the increase of lipophilicity is visible, however the lipophilicity is not the only parameter which influences the activity of the compounds. The mode of action of compounds with similar IC_{50} may differ substantially, depending on the type of derivatization. The role of a sugar moiety as a structural element essential for antimetabolic properties of G21 and **Ram-3** is emphasized by the fact,

Table 4
Cytotoxicity of **Ram-3** and genistein in a panel of cancer cell lines of different origin

Cell line	Organ origin	Ram-3 IC_{50} (μ M)	Genistein IC_{50} (μ M)
SKBR-3 ^a	Breast	28.02 ± 6.89	96.70 ± 4.6
MCF-7 ^a	Breast	8.88 ± 0.75	62.71 ± 15.7
HT-29 ^a	Colon	36.14 ± 4.69	52.78 ± 9.1
Caco-2 ^b	Colon	23.3 ± 3.23	>100
LoVo ^b	Colon	9.85 ± 1.66	15.88 ± 2.4
T98C ^a	Glioblastoma	16.74 ± 10.34	89.41 ± 20.11
DU145 ^b	Prostate	14.45 ± 5.1	47.29 ± 11.78
LNCAp ^a	Prostate	17.98 ± 6.09	30.65 ± 11.15
PC3 ^b	Prostate	10.7 ± 2.27	65.17 ± 12.3
A549 ^a	Lung	14.73 ± 2.23	43.09 ± 7.5
AGS ^b	Stomach	3.05 ± 0.7	41.67 ± 10.4

^a SRB assay.

^b MTT assay.

that the derivative **Gen-5**, obtained through attachment of five C-atoms side chain to C-7 of genistein, which exhibits similar lipophilicity and cytotoxicity as **Ram-3** and, does not affect microtubule network. The lack of toxicity of a sugar moiety (**Ram-P**), and significantly higher toxicity of **Ram-3**, as compared with genistein, and the unique ability of the glycoconjugate to affect microtubules of a spindle indicate, that lipophilic sugar in **Ram-3** does not act simply as a carrier, delivering genistein into cells. The interaction of **Ram-3** with microtubules should be also discussed in the light of the latest paper by Mukherjee et al.,⁴⁸ which shows that genistein is able to depolymerize interphase microtubules through binding to a unique site of tubulin. In this context, it seems possible, that proper derivatization of genistein could enhance genistein intrinsic capability of interaction with microtubules, and concomitantly change this activity of genistein, which blocks cells in G₂ phase and abolishes their entry into mitosis.

The interference with microtubules seems to be dependent both on the sugar moiety and on the length of a spacer between genistein and a sugar residue. Neither **Ram-2** nor **Ram-5**, which differ from **Ram-3** only by the length of a spacer, are able to influence the structure of the mitotic spindle. Another indication on the role of spacer linking the sugar moiety and genistein for the biological activity comes from the comparison of activity of G21 and a series of Lac derivatives (**Lac-2**, **Lac-3**, **Lac-5**), in which the sugar moiety, the same as in G21 is linked to genistein via a C2–C5 spacer. In this case, extension of the distance between the sugar and aglycon led to loss of the antimetabolic activity of Lac derivatives, suggesting, that the size of a molecule may affect its interaction with tubulin.

3.3. Conclusions

Genistein exhibits activity towards multiple molecular targets and reveals potential for affinity TuneUp by derivatization. In our experiments, among genistein modified at C7 by different mono and di-unsaturated sugars, several compounds appeared more active than a parent compound in preliminary screening for inhibition of cancer cell proliferation. The most potent compound, **Ram-3** was capable of influencing the mitotic spindle and inducing apoptosis. For other active genistein glycoconjugates the molecular targets remain to be revealed. We can not exclude their action on the protein targets inhibited by genistein, such as tyrosine kinases and topoisomerases, or new ones, not affected by genistein. Based on our previous⁸ and presently reported results, it is evident that glycoconjugates of genistein containing unsaturated pyranoside moiety, belong to this part of the chemical structure space, which contains islands of pharmacological activity, potentially medicinal useful and applicable for drug development.

Acknowledgments

This work was supported by a grant of Polish Ministry of Science and Higher Education PBZ MNiL-1/1/2005. We would like to acknowledge MSc Katarzyna Ludwik for the study of **Ram-3** stability and MSc Anna Rusek and Ms. Krystyna Klyszcz for excellent technical assistance.

References and notes

- Dixon, R. A.; Ferreira, D. *Phytochemistry* **2002**, *60*, 205.
- Kuiper, G. G.; Lemmen, J. G.; Carlsson, B.; Corton, J. C.; Safe, S. H.; van der Saag, P. T.; van der Burg, B.; Gustafsson, J. A. *Endocrinology* **1998**, *139*, 4252.
- Setchell, K. D.; Brown, N. M.; Desai, P.; Zimmer-Nechemias, L.; Wolfe, B. E.; Brashear, W. T.; Kirschner, A. S.; Cassidy, A.; Heubi, J. E. *J. Nutr.* **2001**, *131*, 1362S.
- Bitto, A.; Burnett, B. P.; Polito, F.; Marini, H.; Levy, R. M.; Armbruster, M. A.; Minutoli, L.; Di Stefano, V.; Irrera, N.; Antoci, S.; Granese, R.; Squadrito, F.; Altavilla, D. *Br. J. Pharmacol.* **2008**, *155*, 896.

5. Banerjee, S.; Li, Y.; Wang, Z.; Sarkar, F. H. *Cancer Lett.* **2008**, *269*, 226.
6. Jakóbkiewicz-Banecka, J.; Piotrowska, E.; Narajczyk, M.; Barańska, S.; Węgrzyn, G. *J. Biomed. Sci.* **2009**, *16*, 26.
7. Rusin, A.; Krawczyk, Z.; Grynkiewicz, G.; Gogler, A.; Zawisza-Puchałka, J.; Szeja, W. *Acta Biochim. Pol.* **2010**, *57*, 23.
8. Rusin, A.; Gogler, A.; Głowala-Kosińska, M.; Bochenek, D.; Gruca, A.; Grynkiewicz, G.; Zawisza, J.; Szeja, W.; Krawczyk, Z. *Bioorg. Med. Chem. Lett.* **2009**, *19*, 4939.
9. Coldham, N. G.; Darby, C.; Hows, M.; King, L. J.; Zhang, A.-Q.; Sauer, M. J. *Xenobiotica* **2002**, *32*, 45.
10. Smith, G. J.; Thomsen, S. J.; Markham, K. R.; Andary, C.; Cardon, D. J. *Photochem. Photobiol.* **2000**, *136*, 87.
11. Setchell, K. D. R.; Brown, N. M.; Zimmer-Nechemias, L.; Brashear, W. T.; Wolfe, B. E.; Kirschner, A. S.; Heubi, J. E. *Am. J. Clin. Nutr.* **2002**, *76*, 447.
12. Steensma, A.; Noteborn, H. P. J. M.; van der Jagt, R. C. M.; Polman, T. H. G.; Mengelers, M. J. B.; Kuiper, H. A. *Environ. Toxicol. Pharmacol.* **1999**, *7*, 209.
13. Kroon, P. A.; Clifford, M. N.; Crozier, A.; Day, A. J.; Donovan, J. L.; Manach, C.; Williamson, G. *Am. J. Clin. Nutr.* **2004**, *80*, 15.
14. Andlauer, W.; Kolb, J.; Stehle, P.; Fürst, P. *J. Nutr.* **2000**, *130*, 843.
15. Zhang, Y.; Song, T. T.; Cunnick, J. E.; Murphy, P. A.; Hendrich, S. *J. Nutr.* **1999**, *129*, 399.
16. Shimoda, K.; Kobayashi, T.; Akagi, M.; Hamada, H. *Chem. Lett.* **2008**, *37*, 876.
17. Polkowski, K.; Popiołkiewicz, J.; Krzeczynski, P.; Ramza, J.; Pucko, W.; Zegrocka-Stendel, O.; Boryski, J.; Skierski, J. S.; Mazurek, A. P.; Grynkiewicz, G. *Cancer Lett.* **2004**, *203*, 59.
18. Popiołkiewicz, J.; Polkowski, K.; Skierski, J. S.; Mazurek, A. P. *Cancer Lett.* **2005**, *229*, 67.
19. Dimri, G. P.; Lee, X.; Basile, G.; Acosta, M.; Scott, G.; Roskelley, C.; Medrano, E. E.; Linskens, M.; Rubelj, I.; Pereira-Smith, O. *Proc. Natl. Acad. Sci. U.S.A.* **1995**, *92*, 9363.
20. Renner, S. G.; Schneider, G. *Chem. Med. Chem.* **2006**, *1*, 181.
21. Mooij, W. T. M.; Hartshorn, M. J.; Tickle, L. J.; Sharff, A. J.; Verdonk, M. L.; Jhoti, H. *Chem. Med. Chem.* **2006**, *1*, 827.
22. Shi, L.; Ge, H.-M.; Tan, S.-H.; Li, H.-Q.; Song, Y.-C.; Zhu, H.-L.; Tan, R.-X. *Eur. J. Med. Chem.* **2007**, *42*, 558.
23. Grynkiewicz, G.; Zegrocka-Stendel, O.; Pucko, W.; Ramza, J.; Koscielcka, A.; Kolodziejcki, W.; Wozniak, K. *J. Mol. Struct.* **2004**, *694*, 121.
24. Ferrier, R. J. *Top. Curr. Chem.* **2001**, *215*, 153.
25. Ferrier, R. J.; Zubkov, O. A. *Org. React.* **2003**, *62*, 569.
26. Ferrier, R. J.; Hoberg, J. O. *Adv. Carbohydr. Chem. Biochem.* **2003**, *58*, 55.
27. Ferrier, R. A. J.; Prasad, N. J. *J. Chem. Soc. C* **1969**, 570.
28. Danishefsky, S.; Keerwin, J. F. J. *Org. Chem.* **1982**, *47*, 3803.
29. Babu, B. S.; Balasubramanian, K. K. *Tetrahedron Lett.* **2000**, *41*, 1271.
30. Das, S. K.; Reddy, K. A.; Roy, J. *Synlett* **2003**, 1607.
31. Yadav, J. S.; Subba Reddy, B. V. *Synthesis* **2002**, *4*, 511.
32. Toshima, K.; Miyamoto, N.; Matsuo, G.; Nakata, M.; Matsumura, S. *Chem. Commun.* **1996**, 1379.
33. Shanmugasundaram, B.; Bose, A. K.; Balasubramanian, K. K. *Tetrahedron Lett.* **2002**, *43*, 6795.
34. de Oliveira, R. N.; de Freitas, J. R.; Srivastava, R. M. *Tetrahedron Lett.* **2002**, *43*, 2141.
35. Grynkiewicz, G.; Priebe, W.; Zamojski, A. *Carbohydr. Res.* **1979**, *68*, 33.
36. Bhate, P.; Horton, D.; Priebe, W. *Carbohydr. Res.* **1985**, *144*, 331.
37. Jordan, M. A.; Thrower, D.; Wilson, L. *Cancer Res.* **1991**, *51*, 2212.
38. Wilson, L.; Jordan, M. A. *Pharmacological Probes of Microtubule Function*. In *Microtubules*; Hyams, J. S., Lloyd, C. W., Eds.; Wiley-Liss: New York, 1994; pp 59–83.
39. Panda, D.; Jordan, M. A.; Chu, K. C.; Wilson, L. *J. Biol. Chem.* **1996**, *271*, 29807.
40. Jordan, M. A.; Thrower, D.; Wilson, L. *J. Cell Sci.* **1992**, *102*, 401.
41. Chen, J. G.; Horvitz, S. B. *Cancer Res.* **2002**, *62*, 1935.
42. Wendell, K. L.; Wilson, L.; Jordan, M. A. *J. Cell Sci.* **1993**, *104*, 261.
43. Guimaraes, G. J.; Dong, Y.; McEwen, B. F.; DeLuca, J. G. *Curr. Biol.* **2008**, *18*, 1778.
44. Saunders, W. *Semin. Cancer Biol.* **2005**, *15*, 25.
45. Kobayashi, Y.; Yonehara, S. *Cell Death Differ.* **2009**, *16*, 139.
46. Castedo, M.; Coquelle, A.; Vivet, S.; Vitale, I.; Kauffmann, A.; Dessen, P.; Pequignot, M. O.; Casares, N.; Valent, A.; Mouhamad, S.; Schmitt, E.; Modjtahedi, N.; Vainchenker, W.; Zitvogel, L.; Lazar, V.; Garrido, C.; Kroemer, G. *EMBO J.* **2006**, *25*, 2584.
47. Margolis, R. L.; Lohez, O. D.; Andreassen, P. R. *J. Cell Biochem.* **2003**, *88*, 673.
48. Mukherjee, S.; Acharya, B. R.; Bhattacharyya, B.; Chakrabarti, G. *Biochemistry* **2010**, *49*, 1702.